BMC Cell Biology

Research article

MID1 and MID2 homo- and heterodimerise to tether the rapamycin-sensitive PP2A regulatory subunit, Alpha 4, to microtubules: implications for the clinical variability of X-linked Opitz GBBB syndrome and other developmental disorders

Kieran M Short[1], Blair Hopwood[1], Zou Yi[1] and Timothy C Cox*[1,2]

Address: [1]Department of Molecular Biosciences & ARC Special Research Centre for the Molecular Genetics of Development, University of Adelaide, Adelaide, South Australia, Australia 5005 and [2]South Australian Clinical Genetics Service, Women's & Children's Hospital, North Adelaide, South Australia, Australia 5006

E-mail: Kieran M Short - kieran.short@adelaide.edu.au; Blair Hopwood - blair.hopwood@adelaide.edu.au; Zou Yi - julie.zou@adelaide.edu.au; Timothy C Cox* - timothy.cox@adelaide.edu.au

*Corresponding author

Published: 4 January 2002

BMC Cell Biology 2002, **3**:1

Received: 5 November 2001
Accepted: 4 January 2002

This article is available from: http://www.biomedcentral.com/1471-2121/3/1

Abstract

Background: Patients with Opitz GBBB syndrome present with a variable array of developmental defects including craniofacial, cardiac, and genital anomalies. Mutations in the X-linked *MID1* gene, which encodes a microtubule-binding protein, have been found in ~50% of Opitz GBBB syndrome patients consistent with the genetically heterogeneous nature of the disorder. A protein highly related to MID1, called MID2, has also been described that similarly associates with microtubules.

Results: To identify protein partners of MID1 and MID2 we undertook two separate yeast two-hybrid screens. Using this system we identified Alpha 4, a regulatory subunit of PP2-type phosphatases and a key component of the rapamycin-sensitive signaling pathway, as a strong interactor of both proteins. Analysis of domain-specific deletions has shown that the B-boxes of both MID1 and MID2 mediate the interaction with Alpha 4, the first demonstration in an RBCC protein of a specific role for the B-box region. In addition, we show that the MID1/2 coiled-coil motifs mediate both homo- and hetero-dimerisation, and that dimerisation is a prerequisite for association of the MID-Alpha 4 complex with microtubules.

Conclusions: Our findings not only implicate Alpha 4 in the pathogenesis of Opitz GBBB syndrome but also support our earlier hypothesis that MID2 is a modifier of the X-linked phenotype. Of further note is the observation that Alpha 4 maps to Xq13 within the region showing linkage to FG (Opitz-Kaveggia) syndrome. Overlap in the clinical features of FG and Opitz GBBB syndromes warrants investigation of Alpha 4 as a candidate for causing FG syndrome.

Background

Opitz GBBB syndrome (OS; Opitz syndrome) is a genetically and phenotypically complex disorder defined by characteristic facial anomalies (hypertelorism and variably labiopalatine and laryngotracheo-esophageal (LTE) clefting), structural heart defects, as well as anal and genital anomalies [1,2]. Recently, we and others identified the *MID1* gene (also called *FXY*) as the underlying cause of

the X-linked form of the disease [3–5]. Defects in *MID1* have been found in ~50% of OS cases consistent with evidence from genetic linkage and cytogenetic studies that at least one autosomal form of the disorder, at chromosome position 22q11.2, also exists [6–8]. The deletion of the same interval produces the 22q11 deletion syndrome, which encompasses a group of disorders (eg. DiGeorge and velocardiofacial syndromes) showing some phenotypic overlap with OS [6,9]. Collectively, 22q11 anomalies represent one of the most common genetic causes of malformations (estimated 1 in 5000 live births) [10]. Although progress has recently been made towards elucidating the genes contributing to the 22q11 deletion phenotype [11–14], a specific autosomal OS gene has not yet been identified.

The *MID1* gene encodes the defining member of a new subclass of the RBCC (RING, B-box, Coiled-Coil) family of proteins. This subclass is characterised by the combination of both a fibronectin type III motif and a B30.2-like (or SPRY) domain positioned C-terminal to the RBCC domain [15,16]. As in other members of the RBCC protein family, MID1 forms multiprotein complexes of between 250 and 450 kDa [17]. The MID1 protein, presumably as part of these complexes, has been shown to associate with cytoplasmic microtubules along their length and throughout the cell cycle using immunofluorescence detection of endogenous MID1, transient expression of GFP-MID1 fusion proteins, and cellular fractionation [5,18]. Most mutations in *MID1* that cause OS are truncating mutations with many, but not all, directly affecting the C-terminal half of the protein [5]. Interestingly, all examined MID1 mutations disrupt the normal microtubule-associated distribution and this has been demonstrated to occur *in vivo* with endogenous mutant protein and in transient transfection studies using GFP fusion proteins [5,17,18].

An intriguing aspect of OS is the marked intrafamilial variability seen even among related males with the same X-linked mutation. This observation may be explained by the fact that other proteins, such as the highly related MID2 protein that is expressed in some of the same tissues and also associates with the microtubule network [15,19], could at least partially compensate for the loss of MID1 [5]. Such a mechanism has also been proposed for other microtubule-associated proteins, such as tau [20]. Alternatively, variations in the level or action of other factors in the same molecular pathway (for example, a factor encoded by the 22q11.2 locus and/or another component of the MID1 macromolecular complex) could contribute to this variability. Both explanations are consistent with the conclusion that OS is caused by loss of function of MID1 [5].

In this paper we report the identification of Alpha 4 as an interacting partner of both the Opitz syndrome protein, MID1, and the highly related MID2 protein. Alpha 4 is a unique and highly conserved regulatory subunit of PP2-type phosphatases, such as PP2A [21–24], and an integral component of the rapamycin-sensitive signaling pathway [25]. Our finding that both MID1 and MID2, either as homo- or hetero-dimers, are able to tether a key regulator of intracellular signaling to microtubules has significant implications for our understanding of the pathophysiological basis of OS and provides additional support for the hypothesis that MID2 could act as a modifier of the OS phenotype. Furthermore, as the *Alpha 4* gene maps to Xq13 [26], our results identify it as a candidate for other X-linked disorders such as FG (Opitz-Kaveggia) syndrome that overlaps clinically with Opitz GBBB syndrome.

Results

Yeast two-hybrid screens identify Alpha 4 as an interacting partner of both MID1 and MID2

In order to begin to determine the identity of potential interacting factors and the processes with which MID1 is involved, we performed a yeast two-hybrid assay utilising the full length MID1 protein (which shares 94.9% identity, 99.9% similarity with mouse Mid1) as bait in a screen of a mouse 10.5 dpc (days post-coitum) whole embryo cDNA library. At 10.5 dpc, expression of *Mid1* is seen essentially throughout the embryo although strongest levels of expression are evident in highly proliferating tissues such as the developing craniofacial region [27]. The use of the mouse 10.5 dpc whole embryo library was therefore chosen to maximise the likelihood of detecting functionally relevant interactors.

Approximately 1×10^6 cDNAs were initially screened using MID1 as bait. Potential interacting clones were selected based on the activation of the three endogenous reporter genes (*His*, *lacZ*, and *Leu*). Recovery and sequencing of the positives from the library screen demonstrated nine cDNA clones with insert sizes ranging from 1.0 kb to 1.3 kb but representing the same gene. Five additional, singly represented putative interacting clones were also identified but do not constitute part of this report. Database searches identified the nine similar clones as encoding Alpha 4, a rapamycin-sensitive regulatory subunit of protein phosphatases 2A (PP2A) and other PP2-type phosphatases. By comparison with the published murine *Alpha 4* sequence, all clones were judged as being essentially full-length. Notably, the nine in-frame cDNAs represented a minimum of seven independent clones as 5' fusion to the GAL4 activation domain occurred at either nucleotide +4, +7, +10 or +13 and most clones containing different length polyadenylated tails. To confirm that this interaction was not an artefact of the independent GAL4 activation domain and DNA binding domain fusion events, the full-length cDNAs were interchanged such that Alpha 4 was fused to the GAL4-DBD and MID1 to GAL4-

A

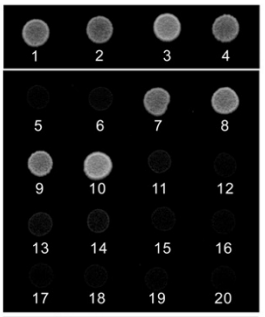

Colony	Interactors
1	pDBLeu-MID1 + pPC86-Alpha4
2	pDBLeu-Alpha4 + pPC86-MID1
3	pDBLeu-MID2 + pPC86-Alpha4
4	pDBLeu-Alpha4 + pPC86-MID2
5	pDBLeu + pPC86
6	pDBLeu + pPC86 (Control A)
7	pDBLeu-Rb + pPC86-Jun (Control B)
8	pDBLeu-Rb + pPC86-E2F1 (Control C)
9	pDBLeu-Jun + pPC86-Jun (Control D)
10	pDBLeu-Fos + pPC86-Jun (Control E)
11	pDBLeu-Alpha4 +pPC86
12	pDBLeu + pPC86-Alpha4
13	pDBLeu-MID1 + pPC86
14	pDBLeu-MID2 + pPC86
15	pDBLeu + pPC86-MID1
16	pDBLeu + pPC86-MID2
17	pDBLeu + pPC86-MID1ΔBB
18	pDBLeu + pPC86-MID1ΔCC
19	pDBLeu + pPC86-MID2ΔBB
20	pDBLeu + pPC86-MID2ΔCC

controls

B

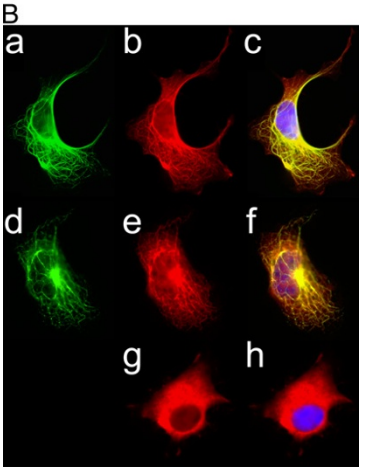

Figure 1
Alpha 4 interacts with MID1 and MID2. (A) Yeast two-hybrid analysis of the interaction between MID1 and Alpha 4 as well as MID2 and Alpha 4. Yeast agar plate (leu$^-$ trp$^-$ his$^-$, 75 mM 3-AT) showing growth for MID1/Alpha 4 and MID2/Alpha 4 interactions as well as positive control two-hybrid combinations and no growth for negative controls. (B) Detection of full-length myc tagged-Alpha 4 when co-expressed with GFP-MID1 and GFP-MID2 fusion proteins in transiently transfected Cos1 cells. (a) GFP-MID1 fluorescence (green), (b) anti-myc antibody detecting myc-Alpha 4 localisation (red), (c) overlay of (a), (b) showing co-localisation of the myc-Alpha 4 fusion protein and GFP-MID1, with DAPI stain for DNA (blue). (d) GFP-MID2 fluorescence (green), (e) myc-Alpha 4 localisation (using same detection as b) (red), (f) overlay of (d), (e) with DAPI (blue) showing co-localisation of the myc-Alpha 4 fusion protein and GFP-MID2. (g) Detection of transiently expressed myc-Alpha 4 fusion protein in Cos1 cells, (h) overlay of (g) and DAPI stain showing cytoplasmic distribution of myc-Alpha 4 fusion protein.

AD. Co-transformation of these two constructs into MaV203 gave similar levels of growth on 3AT (Fig 1A), ie. a level of activation comparable to the strongest interacting proteins, Fos and Jun (Fig 1A, Control E – colony 10).

Given that MID1 and MID2 share 77% overall amino acid identity (92% similarity), we wished to investigate whether MID2 was capable of binding to the same proteins, such as Alpha 4, or whether this interaction was specific for MID1. This was investigated using two approaches: a direct yeast two-hybrid test of the ability of MID2 to bind Alpha 4, and a full two-hybrid screen of the 10.5 dpc whole mouse embryo cDNA library this time using MID2 as bait. The direct test demonstrated that MID2 did indeed interact with Alpha 4. Comparison of the growth of the MID2/Alpha 4 transformed yeast on plates (SC -Leu, -Trp, -His) containing 75 mM 3AT indicated the interaction between MID2 and Alpha 4 was as strong, or stronger, than that observed for MID1 (Fig 1A). A similar result was obtained when assessing the conversion of Xgal (data not shown). In the full yeast two-hybrid screen, some potentially novel interactors were identified for MID2. However, the majority of the putative interacting clones, and again the only sequences represented more than once in the isolates, represented Alpha 4.

MID1 and MID2 tether Alpha 4 to the microtubules

To investigate whether Alpha 4 also associated with MID1 and MID2 in a homologous (mammalian) system, we co-transfected both GFP-MID1 (or MID2) with myc epitope-tagged Alpha 4. Transfection of the myc-tagged Alpha 4 expression construct alone resulted in a diffuse distribution of the myc-Alpha 4 fusion protein throughout the cytoplasm in most cells (Fig 1B; g, h). However, in some cells, a faint filamentous distribution that resembled the appearance of microtubules could be seen along with the cytoplasmic protein (data not shown). In contrast, in all cells co-transfected with GFP-MID1 and myc-tagged Alpha 4, there was negligible diffuse cytoplasmic staining. Instead, essentially all the myc-tagged Alpha 4 protein displayed a filamentous meshwork of staining that completely co-localised with MID1 along the length of the microtubules (Fig 1B; a-c). This result also suggested that MID1 was a limiting factor in the tethering of Alpha 4 to the microtubule network, a conclusion supported by western analysis that shows low levels of MID1 in these cells (data not shown). Co-expression of GFP-MID2 and myc-tagged Alpha 4 similarly resulted in co-localisation along the microtubules (Fig 1B; d-f).

Alpha 4 does not co-localise with MID1 or MID2 proteins harboring in-frame B-box deletions

Both endogenous mutant MID1 protein in OS patient cells [18] and various transiently expressed mutant MID1-GFP fusion proteins form cytoplasmic clumps

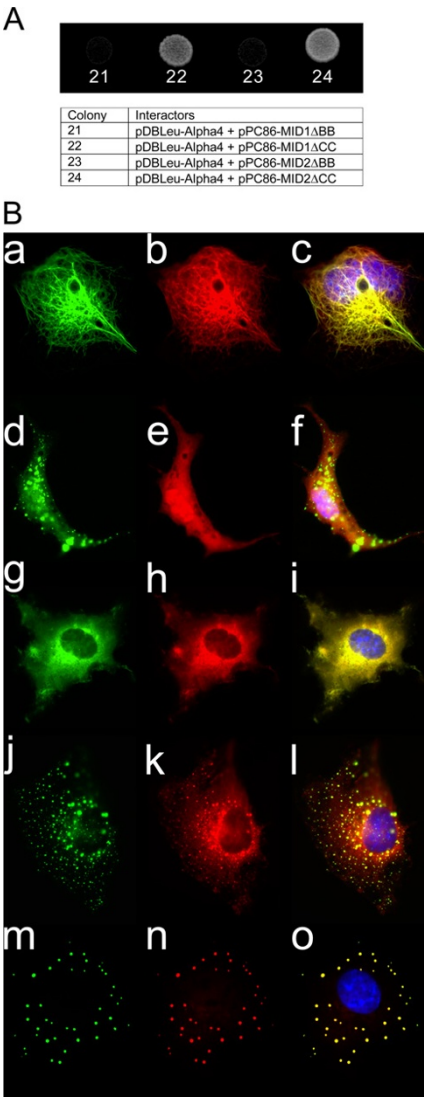

Figure 2
MID1/Alpha 4 and MID2/Alpha 4 interactions are maintained in all MID domain-specific deletions except for those involving the B-boxes. (A) Yeast two hybrid analysis shows that the MID B-boxes are required for interaction with Alpha 4. The interaction of Alpha 4 with MID1ΔBB (21), or MID2ΔBB (23), is compared to its interaction with MID1ΔCC (22), or MID2ΔCC (24). (B) Subcellular localisation of myc tagged-Alpha 4 when co-expressed in Cos-1 cells with MID1 domain-specific deletions as GFP fusion proteins. Fluorescence detection of GFP-MID1ΔRF (a), GFP-MID1ΔBB (d), GFP-MID1ΔCC (g), GFP-MID1ΔFNIII (j), and GFP-MID1ΔCTD (m). Anti-myc antibody detection of myc-Alpha 4 in the same cells as expressing the various MID1 domain-specific deletions (b,e,h,k,n). Overlay of the GFP and anti-myc images of the same cells merged with DAPI stain of nuclei (c,f,i,l,o). All merged images, with the exception of (f) show co-localisation of myc-Alpha 4 with the various MID1 domain deletions. In (f), myc-Alpha 4 fails to co-localise with GFP-MID1ΔBB in small cytoplasmic aggregates.

[5,15,17,18]. We chose to exploit this previous observation by co-transfecting GFP-tagged MID1ΔCTD (or MID2ΔCTD) with a construct expressing a myc-tagged Alpha 4 protein in order to investigate whether Alpha 4 still remained bound to MID1 within such aggregates. The results clearly showed a distribution of myc-Alpha 4 that was indistinguishable from the clumped MID1ΔCTD and MID2ΔCTD truncated proteins, indicating that Alpha 4 indeed aggregates with the truncated MID1 and MID2 proteins (Fig 2B; m-o).

To further define the motif in MID1 (and MID2) responsible for the interaction with Alpha 4, we generated in-frame deletions of all other motifs (Table 1) and fused the resulting clones to GFP. We initially transfected each construct alone to examine the effect of each deletion on the intracellular localisation of the proteins. The results showed that each motif, or at least their conserved spacing or arrangement, was essential for the distribution of MID1 (and MID2) along the length of the microtubules. The distribution of the individual domain deleted MID proteins when transfected alone was indistinguishable from their distributions when transfected along with myc-Alpha 4 (see below). Consequently, the GFP fluorescence images in Fig 2B can also be considered a representation of each distribution pattern in the absence of co-transfected myc-Alpha 4. Like the ΔCTD constructs, deletion of either the B-boxes or the FNIII domain also resulted in cytoplasmic clumps or speckles although these usually appeared smaller and greater in number and the speckles still appeared to co-localise with microtubules (data not shown). Both ΔRING proteins, in contrast, showed variability in their distribution with most transfected cells still showing association along the length of the microtubules. However, the microtubule association of these ΔRING proteins often did not extend to the cell periphery. Notably, deletion of the coiled-coil motif in each protein resulted a diffuse cytoplasmic distribution, suggesting that these proteins had lost their ability to associate with microtubules (see Fig 2B; g-i).

We then individually co-transfected each MID1 (and MID2) deletion construct with myc-Alpha 4 in an attempt to define the domain responsible for the interaction with Alpha 4. Co-transfection of either the ΔRING or ΔFNIII proteins with myc-Alpha 4 (Fig 2B; a-c and j-l, respectively) resulted in co-localisation of Alpha 4 with the abnormally distributed MID1 and MID2 proteins, as seen with the ΔCTD proteins. Co-expression of either ΔCC construct with Alpha 4 resulted in both proteins exhibiting a diffuse cytoplasmic distribution although the pattern of each was still suggestive of the two proteins being able to interact (Fig 2B; g-i). Strikingly, when either of the ΔBB constructs was co-expressed with Alpha 4, the mutant MID1 and MID2 proteins still formed cytoplasmic clumps but, in

Table 1: The *MID1* and *MID2* deletion constructs used in pEGFP-C2 for cellular co-localisation analysis, co-immunoprecipitation and in pPC86/pDBLeu for interaction analysis with Alpha 4. Terms: RF denotes a C3HC4 RING finger; BB denotes C2H2 B-Boxes; CC denotes a Coiled-coil motif; FNIII denotes a Fibronectin Type III domain and CTD denotes a C-terminal domain (encompassing a SPRY domain).

Construct	Amino Acids deleted
Mid1ΔRF	1–69
Mid1ΔBB	71–213
Mid1ΔCC	214–349
Mid1ΔFNIII	370–473
Mid1ΔCTD	483–667
Mid2ΔRF	1–69
Mid2ΔBB	71–213
Mid2ΔCC	214–349
Mid2ΔFNIII	370–473
Mid2ΔCTD	483–686
BB(Mid1)	1–70 and 214–667
CC(Mid1)	1–213 and 350–667
BBCC(Mid1)	1–70 and 350–667

both cases, Alpha 4 remained diffuse in the cytoplasm (Fig 2B; d-f). These results imply that the B-boxes (and/or the linker residues between the B-boxes and RING motifs) are primarily responsible for the interaction with Alpha 4.

To confirm these results, we cloned the MID1 and MID2 domain-deletion constructs in-frame into pPC86 and co-transformed into MaV203 with pDBLeu-Alpha 4. As expected from the immunofluorescence data, activation of all two-hybrid reporter genes, at a level similar to that seen with the full-length MID proteins, was observed with the ΔRING, ΔFNIII and ΔCTD proteins (results not shown), confirming that neither of these domains mediated binding to Alpha 4. Notably, both ΔCC proteins also interacted with Alpha 4 (Fig 2A) suggesting that the two proteins were indeed still interacting in the cytoplasm in the immunofluorescence experiments despite not being associated with microtubules. However, the strength of the interaction between the ΔCC proteins and Alpha 4 appeared to be reduced compared to the full-length, ΔRING, ΔFNIII and ΔCTD (data not shown). In contrast, but again confirming the immunofluorescence result, the ΔBB constructs did not activate reporter gene expression indicating the interaction between Alpha 4 and either MID protein was abolished by removal of this motif (Fig 2A).

The coiled-coil domains of MID1 & MID2 are required for homodimerisation and microtubule binding but not Alpha 4 interaction

Immunoprecipitation experiments have previously shown that MID1 can form homodimers/homomultimers [17]. To investigate whether homodimerisation was a prerequisite for binding Alpha 4 and/or association with the microtubules, we first tested whether MID1 can interact with itself in the context of the yeast two-hybrid system. The results clearly indicated that the MID1-MID1 interaction is strong (Fig 3A). Domain-deletion constructs (in pDBLeu and pPC86 vectors) were then introduced into the yeast two-hybrid system. Unlike the proteins harboring a deletion of either the RING, B-boxes or FNIII motifs, the MID1 protein lacking the coiled-coil motif had significantly reduced capacity to bind the wild-type MID1 protein, inferring that the coiled-coil domain is critical for efficient homodimerisation (result not shown). Assessment of MID1 using the MultiCoil algorithm [28] supports the conclusion of dimer formation (not trimer) and that the first of the two coiled-coils in this domain is largely responsible for this property. Interestingly, the MID1 protein in which the CTD motif was removed also demonstrated a reduced ability to bind the wild-type MID1 in this system, although this effect was not as marked as that seen for the ΔCC proteins. Notably, the yeast two-hybrid and immunofluorescence experiments demonstrate that Alpha 4 can still interact with the MID1 and MID2 ΔCC proteins. This observation indicates that Alpha 4 must be able to interact with MID monomers although its tethering to the microtubule network is dependent on MID dimerisation, that is; the MID proteins only associate with microtubules as dimers.

MID1 & MID2 can form heterodimers on microtubules

Given their high level of identity, we investigated whether MID1 and MID2 can also form heterodimers using the yeast two-hybrid system, immunofluorescence of transiently transfected Cos1 cells and co-immunoprecipitation. Co-transformation of the yeast MaV203 strain with both pDBLeu-MID1 and pPC86-MID2 (or in the reverse vector combination) resulted in high level activation of all reporter genes indicating a strong interaction that was comparable to the strength of the MID1-MID1 homo-interaction (Fig 3A). These findings are contradictory to initial reports from a study by Cainarca et al [17] but have been confirmed in experiments involving transient transfection of GFP-MID1 and myc-MID2 fusion constructs (Fig 3B) as well as by co-immunoprecipitation (Fig 3C). Introduction of individual domain-deletions of MID1 together with full-length or domain-deletion MID2, and vice versa, into Cos1 cells and the yeast strain MaV203 using the relevant constructs showed, as expected, that the coiled-coil motif was largely responsible for mediating this heterodimerisation (data not shown).

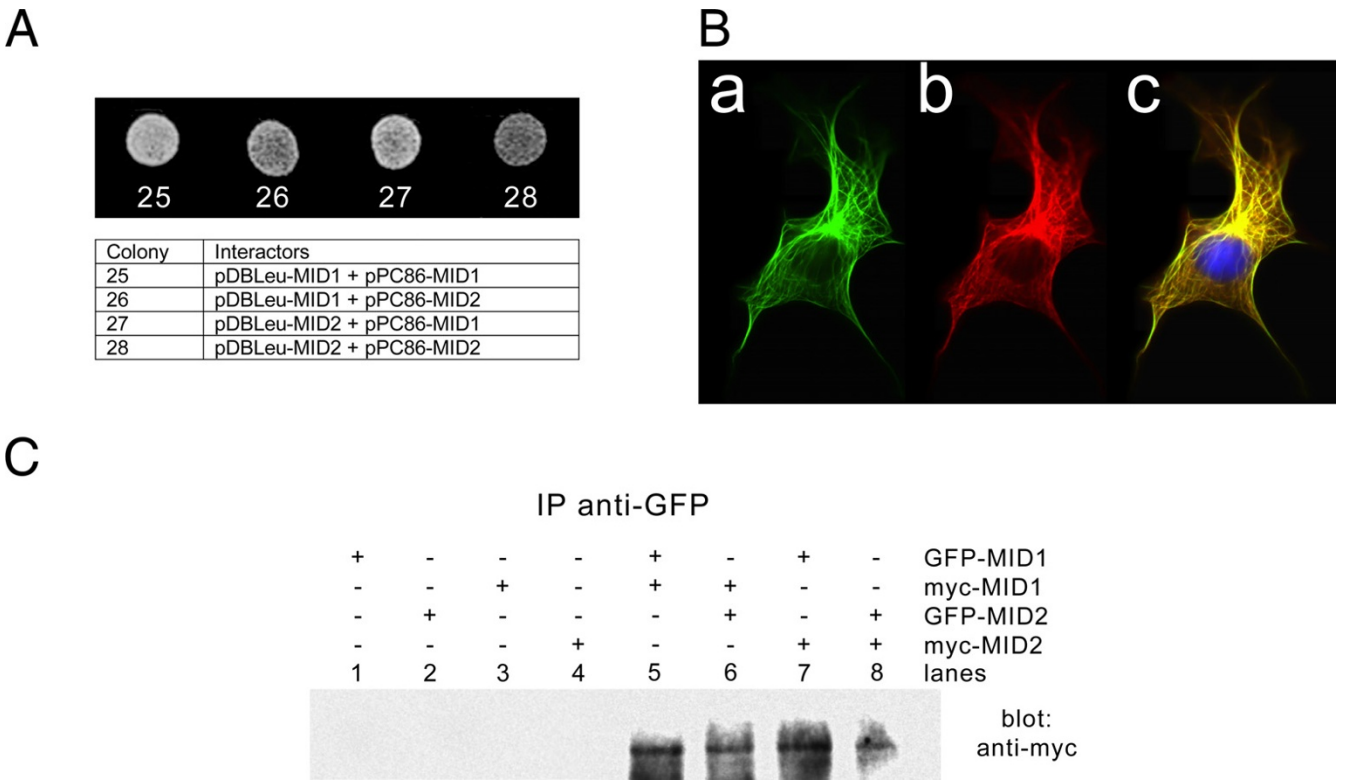

Figure 3
MID1 and MID2 can homo- and heterodimerise with one another. (A) Yeast two-hybrid assay for MID1 and MID2 multimerisation. Yeast agar plate (leu$^-$ trp$^-$ his$^-$, 75 mM 3-AT) showing growth for MID1/MID1 (25), MID1/MID2 (26 and 27) and MID2/MID2 (28). (B) MID1 and MID2 co-localise to the microtubules. Co-expression of GFP-MID1 (a) and myc-MID2 (b) in transiently transfected Cos1 cells showing co-localisation to the microtubular cytoskeleton in an overlay (c) with a DAPI stained nucleus (blue). (C) Co-immunoprecipitation of MID1 and MID2 homo- and heterodimers. Shown are extracts from Cos1 cells, transfected with GFP-MID1 (lane 1), GFP-MID2 (lane 2), myc-MID1 (lane 3), myc-MID2 (lane 4), GFP-MID1 and myc-MID1 (lane 5), GFP-MID2 and myc-MID1 (lane 6), GFP-MID1 and myc-MID2 (lane 7) and GFP-MID2 and myc-MID2 (lane 8). Samples were immunoprecipitated with anti-GFP antibody/protein-A sepharose beads, separated on a 8% SDS polyacrylamide gel, transferred to a nitrocellulose membrane and blotted with anti-c-myc antibody to detect co-precipitate protein.

The B-boxes of MID1 & MID2 are sufficient to bind Alpha 4

To verify that the Alpha 4 interaction and the association of the complex with microtubules were indeed dependent on the B-boxes and coiled-coil, respectively, and not just an artefact of altering the relative spacing of remaining domains, we fused the MID1 B-boxes and coiled-coil motif, or the coiled-coil motif alone, in-frame to GFP and co-transfected with the myc-Alpha 4 construct. Of interest was the observation that the MID1 coiled-coil domain alone fused to GFP (GFP-M1CC) resulted in cytoplasmic clumping (Fig 4B; a), supporting the notion that the coiled-coil domain is required for MID1 dimerisation. Consistent with this is that the phenomenon of cytoplasmic clumping seen in most OS patients has only been observed in those cases where the expressed mutant MID1 protein harbours a mutation outside the coiled coil motif [5]. Notably, however, in cells co-transfected with the GFP-M1CC and myc-Alpha 4 constructs, Alpha 4 did not co-localise with these M1CC clumps (Fig 4B; a-c). Like the M1CC protein, the construct expressing the fusion between GFP and the MID1 B-boxes plus coiled-coil domains (GFP-M1BBCC) resulted in clumps within the cytoplasm. Importantly, and in contrast to the co-transfection of M1CC, Alpha 4 was found to co-localise with the GFP-M1BBCC fusion protein (see Fig 4B; d-f). We did not undertake the generation of a GFP-M1BB (B-boxes alone) construct as it was predicted that the resultant GFP fusion protein would show a diffuse cytoplasmic distribution largely indistinguishable from Alpha 4. Instead, the MID1 B-boxes were cloned into pDBLeu and tested directly for their ability to interact with Alpha 4 in the two-hybrid system. The result (Fig 4A) clearly supports the conclusion that the B-boxes are sufficient to bind Alpha 4.

A

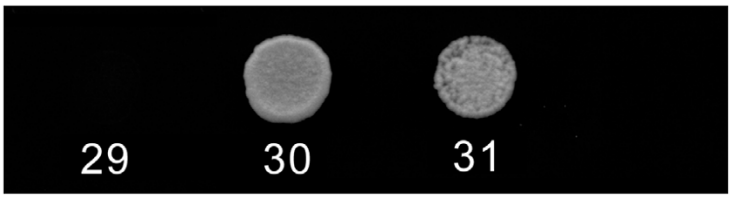

Colony	Interactors
29	pDBLeu + pPC86-M1BB
30	pDBLeu-Alpha4 + pPC86-MID1
31	pDBLeu-Alpha4 + pPC86-M1BB

B

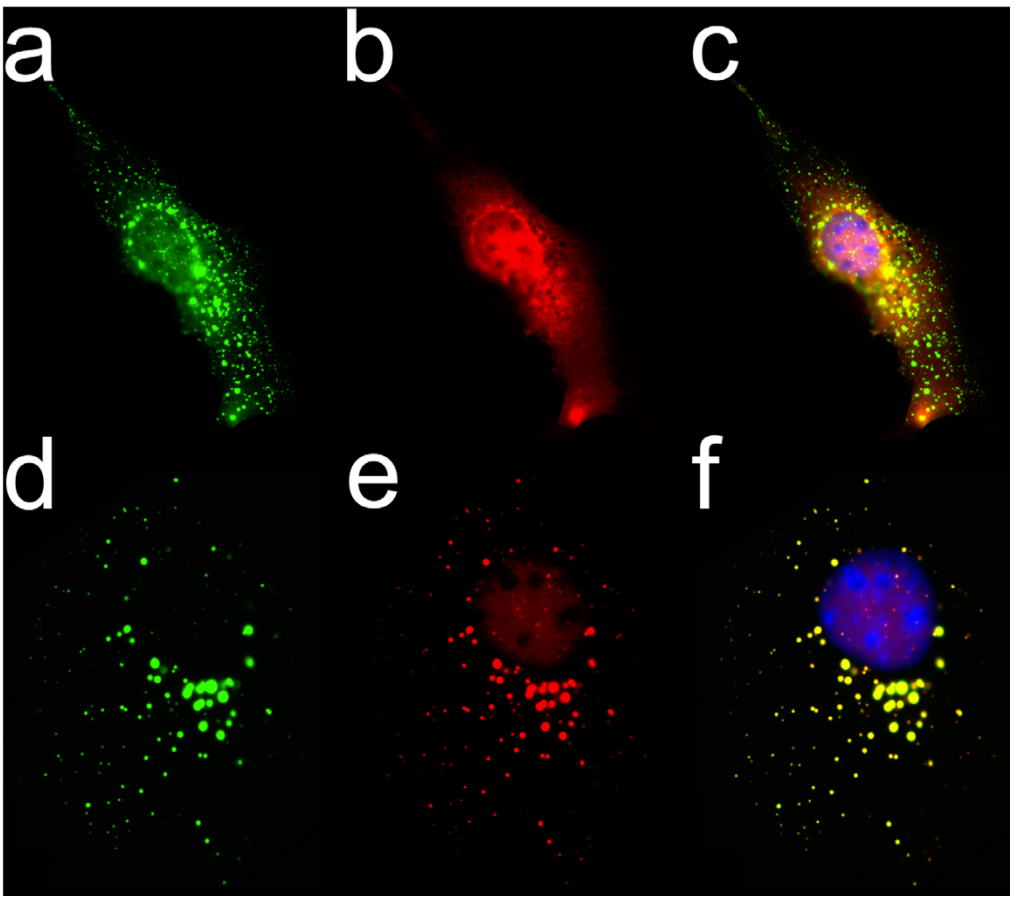

Figure 4
The B-boxes of MID1 are sufficient to bind Alpha 4. (A) Yeast two-hybrid analysis shows that the MID1 B-boxes (pPC86-M1BB) alone can interact with Alpha 4 (pDBLeu-Alpha 4) (31). The wild-type MID1-Alpha 4 interaction (30) and a control with the pPC86-M1BB and no interaction partner (29) were included for comparison. (B) Immunofluorescence assay highlights the importance of the B-boxes for Alpha 4 binding. Subcellular distribution of the GFP-fused MID1 coiled coil domain, GFP-M1CC (a) and myc-Alpha 4 (b) in the same cell shows that the two proteins do not co-localise, as seen in the merged image (c). However, the MID1 fragment, GFP-M1BBCC (d) and the myc-Alpha 4 (e) do co-localise in cytoplasmic speckles as seen in the merged image (f). Both merged images, (c) and (f), also show DAPI stain (blue), which indicates the position of the nucleus.

MID1 is phosphorylated on serine and threonine residues

As Alpha 4 is a regulator of PP2-type serine/threonine phosphatases, we investigated whether MID1 and MID2 might themselves be phosphorylated and hence possible targets of Alpha 4/phosphatase action. Due to the low levels of endogenous MID1 and MID2 in all tested cultured cell lines, we performed western analysis of immunoprecipitated MID-GFP proteins using extracts of Cos1 cells that had been transiently transfected with the various expression constructs. Immunoprecipitation with anti-GFP antibodies followed by western analysis using anti-phosphoserine and anti-phosphothreonine antibodies showed that MID1- and MID2-GFP fusion proteins were phosphorylated on both serine and threonine residues (Fig 5A). Similar analysis using anti-phosphotyrosine antibodies failed to demonstrate phosphorylation of tyrosine residues on either protein (result not shown).

In an attempt to define the location of the sites in MID1 that were phosphorylated, we performed similar immunoprecipitation and western analysis but this time using extracts of Cos1 cells that had been transfected with the individual domain-specific deletion constructs (Fig 5B). That the overall phosphorylation of the MID1 fusion protein was not significantly affected by deletion of any individual domain may suggest that MID1 is phosphorylated at multiple threonine residues along the protein. However, using the anti-phosphoserine antibody, no serine phosphorylation of the ΔBB protein was detected suggesting that most serine phosphorylation in MID1 occurs at or near the B-boxes.

Identification of potential sites of phosphorylation in MID1 and MID2

Computer prediction of potential target residues for phosphorylation by serine/threonine kinases not surprisingly identified numerous consensus sites throughout both human MID1 and MID2. Given the conservation of the rapamycin-sensitive pathway from yeast to mammals and the fact that Alpha 4 binds to both MID1 and MID2 which are only 77% identical, we reasoned that any functionally relevant phosphorylation site should be conserved across species and in both MID1 and MID2 proteins. Examination of available orthologous MID1 and MID2 sequences (from seven and three species, respectively) showed that sixteen of these sites (6 threonines and 10 serines) were fully conserved between all MID proteins (Fig 5C). Interestingly, two of these sites (Ser92 and Ser96), which represent consensus phosphorylation sites for GSK3 and MAPK/CKI/CKII respectively, are the only two conserved serine residues in the amino-terminal half of the protein and, as both are located in the region deleted in the ΔBB constructs of MID1 and MID2, are likely to be the primary sites of serine phosphorylation in these proteins.

Discussion

We have previously shown that the X-linked form of Opitz GBBB syndrome (OS) results from loss of function mutations in *MID1*, a gene that encodes a member of a new class of microtubule-associated proteins [5]. A highly related factor, termed MID2, has also been identified which shares 77% amino acid identity (92% similarity) with MID1 and is expressed in many of the same embryological tissues, albeit at a lower level in most [15,19]. Both MID1 and MID2 are members of the RBCC family of proteins, a group of proteins with diverse intracellular localisations and presumably varied functions. Despite these differences, an ability to function as part of large multiprotein complexes is common to RBCC proteins [29]. Consistent with this is the observation that the 67 kDa MID1 is mostly found in complexes of between 250 kDa and 450 kDa [17]. However, no function has been definitively ascribed to any of the motifs in the MID proteins or indeed either protein as a whole. In this study, we have undertaken yeast two-hybrid screens to identify interacting partners that were likely to constitute part of these MID-complexes as well as performed precise deletion analysis of the MID proteins to begin to elucidate the role of individual motifs.

The only apparent similarity between all the *MID1* mutations identified in patients with OS is that the resultant mutant protein is no longer able to completely decorate the microtubules. This observation implies that the function of one or more proteins within the MID1 complex is absolutely required along the length of the microtubules. Identification of such *bona fide* interactors might therefore be expected to shed light on the possible role of the OS protein and thus provide a better understanding of the molecular pathogenesis of the disorder. To this end, we performed yeast two-hybrid screens using MID1 and MID2 as bait and a 10.5 dpc mouse embryo cDNA library as prey. Significantly, we identified the phosphoprotein, Alpha 4 (also known as IGBP1) as an interactor of both MID proteins. This interaction between the MID proteins and Alpha 4 was confirmed by both vector swapping in the two-hybrid system as well as by co-localisation of differentially tagged proteins to the microtubule network. The specificity of this interaction is also supported by the fact that mouse Mid1 (but not mouse Mid2 presumably because of its lower abundance) was recently identified in the reverse two-hybrid screen of a 9 dpc murine embryonic cDNA library where the mouse Alpha 4 was used as the bait [30]. To characterise this interaction further, we chose to exploit the observation that C-terminal mutations of MID1 form cytoplasmic clumps both *in vivo*[18] and in transformed cell lines over-expressing GFP-mutant MID1 fusion proteins [5,15,17,18] by co-transfecting constructs expressing the ΔCTD proteins (and the other domain-specific deletions of MID1 and MID2) as GFP fusions with

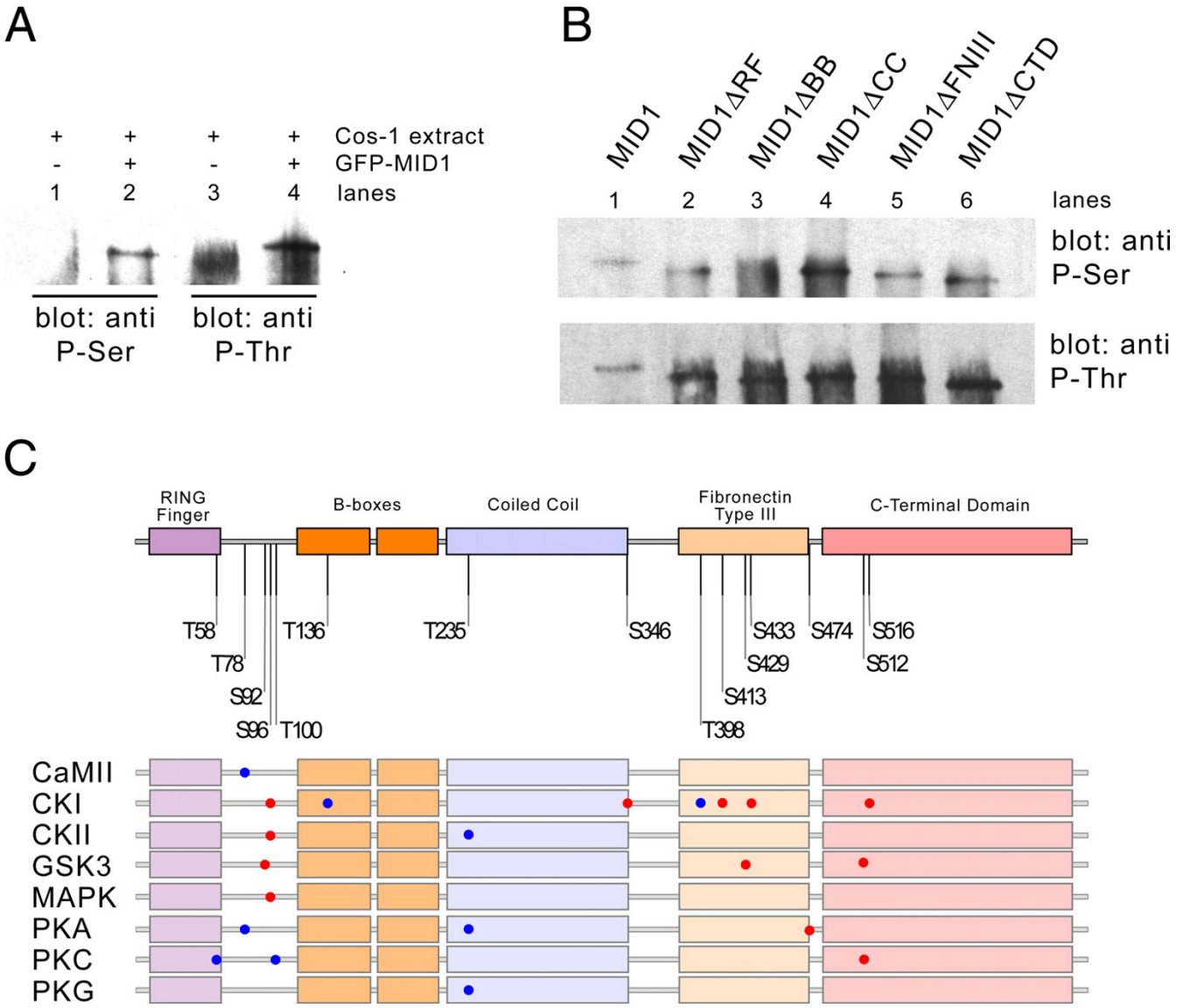

Figure 5
MID1 contains phosphorylated serine and threonine residues. (A) Extracts from untransfected Cos1 cells (lanes 1 & 3) or Cos1 cells transfected with GFP-MID1 (lanes 2 & 4) were immunoprecipitated with anti-GFP antibody/protein-A sepharose beads and analysed by western blot analysis using either an anti-phosphoserine antibody (lanes 1 & 2) or anti-phosphothreonine antibody (lanes 3 & 4). Protein bands in lanes 2 and 4 indicated that GFP-MID1 contains both phosphoserine and phosphothreonine residues. (B) Domain-specific deletions of MID1 were used in an attempt to crudely map locations of the phosphorylated serine and threonine residues. Shown are extracts from Cos1 cells transfected with full length GFP-MID1 (lane 1), GFP-MID1ΔRF (lane 2), GFP-MID1ΔBB (lane 3), GFP-MID1ΔCC (lane 4), GFP-MID1ΔFNIII (lane 5), and GFP-MID1ΔCTD (lane 6). The samples were immunoprecipitated with anti-GFP antibody/-protein-A sepharose beads, separated on 8% SDS polyacrylamide gels, transferred to nitrocellulose membranes and blotted with anti-phosphoserine antibody (top panel) or anti-phosphothreonine antibody (bottom panel). (C) Computer assisted detection of potential serine/threonine phosphorylation sites in MID1. Potential serine/threonine kinase consensus phosphorylation sites in MID1 were identified using NetPhos 2.0 software [38]. Examination of a multiple alignment of available MID1 and MID2 sequences was carried out to identify fully conserved putative phosphorylation sites. A diagrammatic representation of this analysis shows 16 conserved sites depicted as dots (red for serine and blue for threonine) along the length of a representative MID1 protein (numbered residue positions are also depicted at the top of diagram). The actual kinases that recognise the residues are listed on the left of the figure; CaMII (R-X-X-**S**/**T**-X), CKI (Sp/Tp-X_{2-3}-**S**/**T**-X), CKII (X-**S**/**T**-X-X-D/E), GSK3 (X-**S**/**T**-X-X-X-Sp), MAPK (P-X-S/T-P), PKA (R-X_{1-2}-**S**/**T**-X), PKC (X-**S**/**T**-X-R/K), PKG ($(R/K)_{2-3}$-X-**S**/**T**-X).

the myc-tagged Alpha 4 construct. These experiments were complemented by yeast two-hybrid analysis of the same combinations of constructs.

Through a series of in-frame deletions of both MID1 and MID2 employed in both immunofluorescence and yeast two-hybrid assays, we have demonstrated functions for three domains of these RBCC proteins. We have shown a direct role for an RBCC B-box region in protein-protein interactions, that being the binding of Alpha 4, a regulatory subunit of the PP2-type phosphatases including the principal cellular phosphatase, protein phosphatase 2A (PP2A; [21–24]). In addition to the identified role for the B-boxes, we have shown that the coiled-coil domain not only mediates the homodimerisation of these proteins but also their ability to heterodimerise. Finally, our data, together with previous observations by others [18], support a role for the C-terminal domain in microtubule binding and to a lesser extent in dimerisation. Collectively, the immunofluorescence and yeast two-hybrid data indicate that MID dimerisation is a prerequisite for association of each MID-Alpha 4 complex with microtubules.

The interaction of MID1 and MID2 with Alpha 4 raised the possibility that these RBCC proteins, like Xnf7, are phosphoproteins. Indeed, western blot analysis of the transiently expressed MID-GFP fusion proteins using anti-phosphoserine and anti-phosphothreonine antibodies has confirmed these suspicions. Analysis of the domain-specific deletion proteins using these same antibodies showed that most serine phosphorylation of MID1 seems to occur at, or immediately adjacent to, the B-boxes, whereas threonine phosphorylation was likely to occur at residues in more than one domain. As a preliminary step towards identifying those residues that are phosphorylated, computer-based searches identified numerous potential sites for phosphorylation by serine/threonine kinases. However, only sixteen of these (see Fig 5C) are completely conserved across all MID species isolated to date. Of note are the potential phosphorylation sites at serine 96 (S96; [30]) and serine 92 (S92) that are located immediately amino-terminal to the B-boxes of MID1 and MID2 and are deleted in the ΔBB constructs. S92 is a consensus site for GSK3 that would be dependent on prior phosphorylation of S96. S96 falls within a consensus phosphorylation sequence for the MAP-kinase (MAPK), ERK2 (P-N-S/T-P; [31]), as well as casein kinases I and II. Therefore, either of these kinases could conceivably play a priming role for GSK3 phosphorylation of S92. Similar phosphorylation mechanisms have been observed for other proteins including some microtubule-associated proteins, eg. tau and MAP2, where it has been implicated in the regulation of specific functions of those proteins [32,33]. Notably, in the case of both eIF2Bepsilon (at serine residues 535 & 539) and tau (at serine residues 208 & 212), DYRK, a MAPK-related kinase, plays such a priming role for GSK3 [34]. However, DYRK is unlikely to be involved in phosphorylation of MID1 S96 because of a single amino acid difference in its surrounding sequence required for recognition of this site for phosphorylation. In fact, Liu et al [30] have provided evidence to support the involvement of a MAPK, although the target of this activity was not shown. Irrespective of the identity of the kinase(s) responsible, it is conceivable that phosphorylation at these or other sites in MID1 and MID2 could play an important role in the overall function of the MID proteins, for example: regulation of the Alpha 4-MID interaction and hence regulation of PP2-type phosphatase activity. However, our preliminary analysis of a MID1 Ser92/Ser96 double mutant has suggested that MID dimerisation and the MID-Alpha 4 interaction are not dependent on phosphorylation at these residues (unpublished observations).

Regardless of the role of MID phosphorylation, the implication of both MID1 and MID2 in the Alpha 4-mediated regulation of phosphatase activity may provide valuable clues as to the pathophysiological consequences of MID1 mutations that underlie Opitz syndrome. It can be envisaged that, in tethering Alpha 4 to the microtubules, MID1 (and MID2) could be affecting the activity of the PP2-type phosphatases and thereby, in-turn, modulating the rapamycin-sensitive signaling pathway. This could conceivably occur by one of a number of mechanisms. Firstly, the MID proteins may control the availability of Alpha 4 to the phosphatases either by its 1) sequestration or 2) turnover, facilitated by the possible role of the MID RING finger motif in ubiquitination. Secondly, the Alpha 4-MID interaction may direct PP2A (and PP2-related) phosphatase activity to specific targets on the microtubules, which may include MID1 and MID2 themselves. The fact that both endogenous MID1 and transiently expressed GFP-MID1 and GFP-MID2 decorate microtubules throughout the cell cycle ([17]; unpublished observations) suggests that binding of MID1 and MID2 to the microtubule network may not itself be regulated by targeted Alpha 4-dependent PP2A activity. However, it remains possible that dynamic regulation of MID1 microtubule binding may escape detection by immunofluorescence as endogenous levels of MID1 and Alpha 4 in examined cell lines are both low (unpublished observations). The fact that we have not been able to demonstrate PP2A(C) co-localisation with the MID-Alpha 4 complexes on the microtubules, despite a known microtubule-associated pool of PP2A [35], would perhaps support the former of these mechanisms. However, we cannot exclude the possibility that recognition of PP2A(C) by this antibody is blocked by the interaction of Alpha 4 and MID1/2. If this is indeed the case, then it could be envisaged that PP2A(C) is also a target of MID RING-mediated degradation through its in-

dependent interaction with Alpha 4. An alternate hypothesis is that MID function is indeed controlled by Alpha 4-PP2-type phosphatases but through the regulated binding of additional factors that might be components of the MID1 macromolecular complexes. The characterisation of additional interacting partners will therefore be important to assess this possibility.

Numerous studies in mice have demonstrated that Alpha 4, like its yeast homologue Tap42, plays an essential regulatory role within the cell through its regulated binding to the catalytic (C) subunit of PP2-type serine/threonine protein phosphatases [21–24]. The interaction of Alpha 4 with PP2A(C) has been most extensively studied and shown to be dependent on phosphorylation of Alpha 4 by the mTOR (target of rapamycin) kinase. Although PP2A has a wide range of biological functions, Alpha 4 regulates a distinct subset of events in a rapamycin-sensitive manner, including progression through the cell cycle and the regulation of protein biosynthesis (for a review see [36]). The implication that disruption to some aspects of this rapamycin-sensitive pathway might be associated with the pathogenesis of the developmental disorder, Opitz syndrome, raises two intriguing possibilities. Firstly, it can be envisaged that mutations in other components of the pathway may give rise to similar clinical phenotypes. It is therefore perhaps worthy to note that the Alpha 4 gene maps to Xq13 [26] in the vicinity of the critical interval for FG syndrome, a malformation disorder with some clinical overlap with that of Opitz GBBB syndrome. We are currently investigating whether molecular defects in Alpha 4 indeed underlie FG syndrome or other developmental disorders mapping to the proximal long arm of the X chromosome. Secondly, it is also feasible that genetic polymorphisms that reflect a variation in the level of expression or activity of one or more components of the rapamycin-sensitive pathway might also contribute to the clinical variability of OS. In this regard, the indication from our immunofluorescence studies that the microtubular localisation of Alpha 4 is likely to be limited by the level of the MID1 and MID2 proteins within a particular cell type provides indirect support for our earlier hypothesis that MID2 may be able to compensate, at least partially, for the loss of MID1 in Opitz syndrome [5].

Conclusions

The finding that Alpha 4, a rapamycin-sensitive regulatory subunit of PP2-type phosphatases, interacts strongly with the RBCC proteins, MID1 and MID2, implicates this signaling pathway in the pathogenesis of the X-linked form of Opitz GBBB syndrome and provides a possible explanation for the intrafamilial variability in clinical presentation of the disorder. Other components of the rapamycin-sensitive pathway should be considered as candidates for similar malformation disorders.

Materials & Methods

Miscellaneous enzymes and chemicals

All restriction endonucleases were purchased from New England Biolabs (Genesearch Pty Ltd, Arundel, Queensland), Klenow fragment from GeneWorks Pty Ltd (Thebarton, South Australia), and both T4 ligase and T4 DNA polymerase from Roche Diagnostics Australia (Castle Hill, New South Wales). 4',6-diamidine-2-phenylindole' dihydrochloride (DAPI) and 3-Amino Triazole (3AT) were obtained from Sigma-Aldrich (Castle Hill, New South Wales).

The yeast two-hybrid screen

The ProQuest™ yeast two-hybrid system (Invitrogen, Mulgrave, NSW) was employed to screen for potential interacting partners of MID1. In order to generate the "bait" construct, the full-length human MID1 cDNA was subcloned from pBSMID1 [5] using SalI and NcoI into the similarly restricted pDBLeu vector. Subsequent digestion with SalI, end-filling with Klenow fragment and religation generated the full-length MID1 cDNA in-frame with the GAL4 DNA binding domain (Gal4DBD). The construct, pDBLeu-MID1, was verified by sequencing.

The selection of an appropriate cDNA library was deemed critical to maximise the chance of detecting *bona fide* interacting factors. The expression of the murine *Mid1* gene during embryological development is consistent with the clinical presentation of OS [27]. Given the very high level of primary sequence identity between all vertebrate MID1 proteins (unpublished data), a murine 10.5 dpc whole embryo cDNA library (Invitrogen) directionally cloned in the GAL4 activation domain (GAL4-AD) plasmid, pPC86, was selected for use as the "prey" in the two-hybrid screen.

The pDBLeu-MID1 construct was transformed into MaV203 strain (Genotype: *MAT*α, *leu*2–3, 112, *trp*1–901, *his*3Δ200, *ade*2–101, *gal*4Δ, *gal*80Δ, *SPAL*10::*URA*3, *GAL*1::*lacZ*, $HIS3_{UAS\ GAL1}$::*HIS*3@*LYS*2, *can*1^R, *cyh*2^R) along with the parental pPC86 plasmid as per the manufacturers instructions (Invitrogen). The HIS3 reporter was used to determine the level of self-activation of the MID1-GAL4DBD fusion based on the level of 3-amino triazole resistance (3AT^R) of the fusion protein. A concentration of 50 mM 3AT was found to be an adequate level for the assay, although subsequent analyses were performed on 75 mM 3AT plates to further reduce background transactivation of the reporter genes. To screen for potential interacting proteins, the pDBLeu-MID1 fusion construct was co-transformed with the 10.5 dpc mouse embryo cDNA-pPC86 library according to standard protocols (ProQuest™ Yeast Two-Hybrid Manual, Invitrogen) and plated on a synthetic complete medium (SC-Leu-Trp-His) containing either 50 mM or 75 mM 3AT.

The full-length MID2 (FXY2) cDNA was cloned from pEGFP-FXY2.ORF [15] into pDBLeu using the same strategy as used for MID1. As *Mid2* is generally expressed in many of the same tissues during embryological development as *Mid1* albeit at considerably lower levels [19], the resultant clone, pDBLeu-MID2, was consequently used as "bait" in a similar screen of the 10.5 dpc embryo cDNA library as well as directly against the identified MID1 interacting clones.

For confirmation of putative interacting clones, constructs and library clone isolates (in both parental vectors and swapped vectors) were re-transformed into the MaV203 yeast strain using the LiAc method [37]. Transformed yeast cultures were incubated for 24 hours at 30°C in selective media. Cultures (10 µl – 0.1 OD_{600}) were then spotted onto selective plates and incubated at 30°C for 48 hours. Replica cleaning of plates was performed as required.

Generation of GFP- and myc-full-length cDNA fusion constructs for immunofluorescence

The generation of full-length MID1-GFP and MID2-GFP fusions in pEGFP have previously been reported [15,5]. A vector for the production of myc-tagged fusion proteins was generated by modification of the pEGFP-N2 vector (Clontech, Palo Alto, CA). Briefly, the GFP coding region was excised from pEGFP-N2 with NotI and BamHI, the 5' overhangs filled using T4 DNA polymerase and the vector religated to give pCMV-N2. Six copies of the myc epitope containing a start codon was amplified from pGEM-6mycT (gift from M. Whitelaw, University of Adelaide), and cloned into the HindIII site of pCMV-N2. To facilitate in-frame insertion of cDNAs directly from the pPC86 library vector, the plasmid was linearised with EcoRI, end-filled and re-ligated to create pCMV-6myc-ΔE. In order to clone Alpha 4 into pCMV-6myc-ΔE, pPC86-Alpha 4 was digested with SalI/AatII and the full-length cDNA insert ligated into SalI/SmaI restricted pCMV-6Myc-ΔE vector. The reading frame of the construct was confirmed by automated sequencing.

Generation of MID1 and MID2 domain-specific deletion constructs for immunofluorescence and yeast two-hybrid analyses

The FNIII domain-specific deletions in both MID1 and MID2 were generated by precise deletion of the domains by a two-step PCR strategy. The other domain-specific deletion constructs were generated using QuickChange™ site-directed mutagenesis (Stratagene, La Jolla, CA) to introduce unique restriction sites, as required, at the start and end of each domain within MID1 and MID2. Exceptions to this were the RING and B-box deletions of MID1 where a native XbaI site located at nucleotides +207–212 was used as the 3' and 5' excision point in the respective constructs, and the CTD deletions in both MID1 and MID2 where a native BamHI site located at nucleotides +1464–1469 was used as the 5' excision point for these constructs. Restriction sites were chosen so that, where possible, the encoded amino acid sequence remained unaltered or only resulted in conservative substitutions. Furthermore, the sites were positioned such that excision of individual domains did not alter the reading frame of the encoded protein (Table 1). In any one construct, a maximum of two restriction sites were introduced. Details of the strategies and primers (for both PCR and site-directed mutagenesis) used in the generation of these deletion constructs will be forwarded upon request to the corresponding author. Each introduced restriction site was confirmed by digestion and sequencing and then independently tested for its effect on the microtubule binding capacity of the respective proteins. In each case, this was determined by direct visualisation of fluorescence of the created GFP fusion protein. No introduced change had any appreciable effect on the microtubular distribution of the proteins.

To further test the function of some of the regions of the MID1 protein, selected separate motifs were generated using the appropriate existing, and/or inserted, restriction sites and ligated in-frame and C-terminal to either EGFP (in pEGFP) or Gal4DBD (in pDBLeu). The following constructs were generated: the MID1 B-box fusion (pDBLeu-M1BB) containing residues 71–213, the MID1 coiled-coil fusion (pEGFP-M1CC) containing residues 214–349, and the MID1 B-boxes plus coiled-coil fusion (pEGFP-M1BBCC) containing residues 71–349.

Transfection and immunofluorescence analysis of GFP-MID1 constructs

Preparations of the various GFP- and myc-tagged expression constructs were made using the Qiagen Midi kit (Qiagen, Clifton Hill, Victoria). Two picomoles (approximately 1 microgram) of each construct were transfected into cultured cell lines (Cos1, HeLa, NIH3T3) using FuGene transfection reagent (Roche Diagnostics Australia). Transfected cells were grown on coverslips in DMEM plus 10% FBS and fixed 24 hours post-transfection as previously described [5].

In test transfections, where only a single GFP expression construct was introduced into cells, control microtubule staining was performed post-fixation using an anti-α tubulin antibody plus an anti-mouse Texas Red-conjugated secondary antibody (Jackson Laboratories, Bar Harbor, Maine). In cells transfected with myc-tagged expression constructs (either alone or in combination with a GFP-tagged expression construct), anti-α tubulin staining was not performed. Instead the Texas Red-conjugated secondary antibody was used in combination with an anti-myc

monoclonal antibody (9E10) to detect the expression of the myc-tagged protein. In all cases, nuclei were stained using the DNA-specific stain, DAPI. GFP and Texas Red fluorescence were visualised under appropriate wavelength light on an Olympus AX70 microscope. Images were captured using a Photometrics CE200A Camera Electronics Unit and processed using Photoshop 6.01 software (Adobe Systems Incorporated, San Jose, California).

Immunoprecipitation and western analysis

Preparations of the various GFP- and myc-tagged expression constructs were made using a DNA plasmid Midi kit (Qiagen). Six picomoles (approximately 3 micrograms) of each construct were transfected into approximately 10^7 Cos1 cells using FuGene transfection reagent (Roche Diagnostics Australia). After 24 hours incubation, cells were scraped from the culture dish and lysed on ice for 30 minutes in 1 ml lysis buffer (50 mM Tris-Hcl pH 7.4, 300 mM NaCl, 5 mM EDTA, 1.0 % Triton X-100). Cell lysates was cleared by centrifugation at 4°C (15 minutes, 16 ×g), and protein extract recovered as supernatant. After pre-clearing 200 µl of protein extract with 10 µl of 50% protein-A sepharose bead slurry, extracts were incubated with 1 µg of antibody for 2 hours at 4°C and then for another 2 hours with 20 µl of fresh 50% protein-A sepharose bead slurry. The beads were washed four times with wash buffer (50 mM Tris-Hcl pH 7.4, 300 mM NaCl, 5 mM EDTA, 0.1% Triton X-100) and protein eluted from the beads by boiling in 2 × SDS load buffer. Proteins were separated by 8% SDS PAGE and blotted onto Hybond-C membranes (Amersham Pharmacia) using a semi-dry transfer apparatus (BioRad). Membranes were blocked, incubated with the appropriate primary antibody, washed, incubated with the appropriate HRP-conjugated secondary antibody and washed again according to established method described in Current Protocols in Cell Biology. Detection was carried out using an enhanced chemiluminescence reagents (ECL) kit (Amersham Pharmacia) as per the manufacturer's instructions. Antibodies used in immunoprecipitation and western blot analysis included; rabbit polyclonal anti-GFP antibody (gift from Pam Silver, Dana-Farber Cancer Institute, Boston), mouse anti-c-myc monoclonal antibody (gift from Stephen Dalton, University of Adelaide), rabbit polyclonal anti-phosphoserine and anti-phosphothreonine antibodies (Zymed) and HRP conjugated anti-rabbit and anti-mouse secondary antibodies (Amersham Pharmacia).

Computer-assisted detection of serine/threonine phosphorylaton sites

Analysis of putative consensus serine/threonine phosphorylation sites in MID1 was performed using NetPhos version 2.0 [http://www.cbs.dtu.dk/services/NetPhos/] software [38]. Examination of a multiple sequence alignment of all available MID1 and MID2 sequences was performed in order to determine if any putative phosphorylation site was fully conserved. For this analysis, orthologous MID1 sequences were assessed from a variety of species, including human, mouse, rat, chick, tammar wallaby, zebrafish (partial sequence only) and fugu, and MID2 orthologous sequences from human, mouse and rat (partial sequence only).

Note Added In Proof

During the review of this manuscript, a paper by Trockenbacher *et al* [Trockenbacher A, Suckow V, Foerster J, Winter J, Krauβ S, Roper H-H, Schneider R. and Schweiger S: **MID1, mutated in Opitz syndrome, encodes an ubiquitin ligase that targets phosphatase 2A for degradation.** *Nature Genetics* 2001, **29**:287–294] independently reported the interaction of Alpha 4 and MID1. These investigators also showed that MID1, possibly through Alpha 4, regulates the turnover of the microtubule-associated fraction of PP2AC and hence may represent a possible pathological mechanism for the Opitz syndrome phenotype.

Acknowledgements

We would like to thank Professor David Brautigan for kindly sharing data prior to publication. This work was supported by project grant #157958 and in part by an R. Douglas Wright Award (#997706) (to T.C.C.) from the National Health and Medical Research Council of Australia.

References

1. Opitz JM: **G syndrome (hypertelorism with esophageal abnormality and hypospadias, or hypospadias-dysphagia, or "Opitz-Frias" or "Opitz-G" syndrome) – perspective in 1987 and bibliography.** *American Journal of Medical Genetics* 1987, **28**:275-285
2. Robin NH, Opitz JM, Muenke M: **Opitz G/BBB syndrome: clinical comparisons of families linked to Xp22 and 22q, and a review of the literature.** *American Journal of Medical Genetics* 1996, **62**:305-317
3. Quaderi NA, Schweiger S, Gaudenz K, Franco B, Rugarli EI, Berger W, Feldman GJ, Volta M, Andolfi G, Gilgenkrantz S, Marion RW, Hennekam RC, Opitz JM, Muenke M, Ropers HH, Ballabio A: **Opitz G/BBB syndrome, a defect of midline development, is due to mutations in a new RING finger gene on Xp22.** *Nature Genetics* 1997, **17**:285-291
4. Gaudenz K, Roessler E, Quaderi N, Franco B, Feldman G, Gasser DL, Wittwer B, Horst J, Montini E, Opitz JM, Ballabio A, Muenke M: **Opitz G/BBB syndrome in Xp22: mutations in the MID1 gene cluster in the carboxy-terminal domain.** *American Journal of Human Genetics* 1998, **63**:703-710
5. Cox TC, Allen LR, Cox LL, Hopwood B, Goodwin B, Haan E, Suthers GK: **New mutations in MID1 provide support for loss of function as the cause of X-linked Opitz syndrome.** *Human Molecular Genetics* 2000, **9**:2553-2562
6. Robin NH, Feldman GJ, Aronson AL, Mitchell HF, Weksberg R, Leonard CO, Burton BK, Josephson KD, Laxova R, Aleck KA: **Opitz syndrome is genetically heterogeneous, with one locus on Xp22, and a second locus on 22q11.2.** *Nature Genetics* 1995, **11**:459-461
7. McDonald-McGinn DM, Driscoll DA, Bason L, Christensen K, Lynch D, Sullivan K, Canning D, Zavod W, Quinn N, Rome J: **Autosomal dominant "Opitz" GBBB syndrome due to a 22q11.2 deletion.** *American Journal of Medical Genetics* 1995, **59**:103-113
8. Fryburg JS, Lin KY, Golden WL: **Chromosome 22q11.2 deletion in a boy with Opitz (G/BBB) syndrome.** *American Journal of Medical Genetics* 1996, **62**:274-275
9. McDonald-McGinn DM, Tonnesen MK, Laufer Cahana A, Finucane B, Driscoll DA, Emanuel BS, Zackai EH: **Phenotype of the 22q11.2 deletion in individuals identified through an affected relative: cast a wide FISHing net!** *Genet Med* 2001, **3**:23-29

10. Glover TW: **CATCHing a break on 22.** *Nature Genetics* 1995, **10**:257-258
11. Guris DL, Fantes J, Tara D, Druker BJ, Imamoto A: **Mice lacking the homologue of the human 22q11.2 gene CRKL phenocopy neurocristopathies of DiGeorge syndrome.** *Nature Genetics* 2001, **27**:293-298
12. Jerome LA, Papaioannou VE: **DiGeorge syndrome phenotype in mice mutant for the T-box gene, Tbx1.** *Nature Genetics* 2001, **27**:286-291
13. Lindsay EA, Vitelli F, Su H, Morishima M, Huynh T, Pramparo T, Jurecic V, Ogunrinu G, Sutherland HF, Scambler PJ, Bradley A, Baldini A: **Tbx1 haploinsufficieny in the DiGeorge syndrome region causes aortic arch defects in mice.** *Nature* 2001, **410**:97-101
14. Merscher S, Funke B, Epstein JA, Heyer J, Puech A, Lu MM, Xavier RJ, Demay MB, Russell RG, Factor S, Tokooya K, Jore BS, Lopez M, Pandita RK, Lia M, Carrion D, Xu H, Schorle H, Kobler JB, Scambler P, Wynshaw-Boris A, Skoultchi AI, Morrow BE, Kucherlapati R: **TBX1 is responsible for cardiovascular defects in velo-cardio-facial/ DiGeorge syndrome.** *Cell* 2001, **104**:619-629
15. Perry J, Short KM, Romer JT, Swift S, Cox TC, Ashworth A: **FXY2/ MID2, a gene related to the X-linked Opitz syndrome gene FXY/MID1, maps to Xq22 and encodes a FNIII domain-containing protein that associates with microtubules.** *Genomics* 1999, **62**:385-394
16. Short KM, Hopwood B, Cox TC: **Further subdivision of the RBCC family of proteins defined by the presence of a Fibronectin type III motif.** *in preparation*
17. Cainarca S, Messali S, Ballabio A, Meroni G: **Functional characterization of the Opitz syndrome gene product (midin): evidence for homodimerization and association with microtubules throughout the cell cycle.** *Human Molecular Genetics* 1999, **8**:1387-1396
18. Schweiger S, Foerster J, Lehmann T, Suckow V, Muller YA, Walter G, Davies T, Porter H, van Bokhoven H, Lunt PW, Traub P, Ropers HH: **The Opitz syndrome gene product, MID1, associates with microtubules.** *Proceedings of the National Academy of Sciences of the United States of America* 1999, **96**:2794-2799
19. Buchner G, Montini E, Andolfi G, Quaderi N, Cainarca S, Messali S, Bassi MT, Ballabio A, Meroni G, Franco B: **MID2, a homologue of the Opitz syndrome gene MID1: similarities in subcellular localization and differences in expression during development.** *Human Molecular Genetics* 1999, **8**:1397-1407
20. Takei Y, Teng J, Harada A, Hirokawa N: **Defects in axonal elongation and neuronal migration in mice with disrupted tau and map1b genes.** *Journal of Cell Biology* 2000, **150**:989-1000
21. Chen J, Peterson RT, Schreiber SL: **Alpha 4 associates with protein phosphatases 2A, 4, and 6.** *Biochemical and Biophysical Research Communications* 1998, **247**:827-832
22. Inui S, Sanjo H, Maeda K, Yamamoto H, Miyamoto E, Sakaguchi N: **Ig receptor binding protein 1 (alpha4) is associated with a rapamycin-sensitive signal transduction in lymphocytes through direct binding to the catalytic subunit of protein phosphatase 2A.** *Blood* 1998, **92**:539-546
23. Murata K, Wu J, Brautigan DL: **B cell receptor-associated protein alpha4 displays rapamycin-sensitive binding directly to the catalytic subunit of protein phosphatase 2A.** *Proceedings of the National Academy of Sciences of the United States of America* 1997, **94**:10624-10629
24. Nanahoshi M, Tsujishita Y, Tokunaga C, Inui S, Sakaguchi N, Hara K, Yonezawa K: **Alpha4 protein as a common regulator of type 2A-related serine/threonine protein phosphatases.** *FEBS Letters* 1999, **446**:108-112
25. Schmelzle T, Hall MN: **TOR, a central controller of cell growth.** *Cell* 2000, **103**:253-262
26. Onda M, Inui S, Maeda K, Suzuki M, Takahashi E, Sakaguchi N: **Expression and chromosomal localization of the human alpha 4/IGBP1 gene, the structure of which is closely related to the yeast TAP42 protein of the rapamycin-sensitive signal transduction pathway.** *Genomics* 1997, **46**:373-378
27. Dal Zotto L, Quaderi NA, Elliott R, Lingerfelter PA, Carrel L, Valsecchi V, Montini E, Yen CH, Chapman V, Kalcheva I, Arrigo G, Zuffardi O, Thomas S, Willard HF, Ballabio A, Disteche CM, Rugarli EI: **The mouse Mid1 gene: implications for the pathogenesis of Opitz syndrome and the evolution of the mammalian pseudoautosomal region.** *Human Molecular Genetics* 1998, **7**:489-499
28. Wolf E, Kim PS, Berger B: **a program for predicting two- and three-stranded coiled coils.** *Protein Science* 1997, **6**:1179-1189
29. Borden KL: **RING fingers and B-boxes: zinc-binding protein-protein interaction domains.** *Biochemistry and Cell Biology* 1998, **76**:351-358
30. Liu J, Prickett TD, Elliott E, Meroni G, Brautigan DL: **Phosphorylation and microtubule association of the Opitz syndrome protein mid-1 is regulated by protein phosphatase 2A via binding to the regulatory subunit alpha 4.** *Proceedings of the National Academy of Sciences of the United States of America* 2001, **98**:6650-6655
31. Himpel S, Tegge W, Frank R, Leder S, Joost HG, Becker W: **Specificity determinants of substrate recognition by the protein kinase DYRK1A.** *Journal of Biological Chemistry* 2000, **275**:2431-2438
32. Chu B, Soncin F, Price BD, Stevenson MA, Calderwood SK: **Sequential phosphorylation by mitogen-activated protein kinase and glycogen synthase kinase 3 represses transcriptional activation by heat shock factor-1.** *Journal of Biological Chemistry* 1996, **271**:30847-30857
33. Sanchez C, Perez M, Avila J: **GSK3beta-mediated phosphorylation of the microtubule-associated protein 2C (MAP2C) prevents microtubule bundling.** *European Journal of Cell Biology* 2000, **79**:252-260
34. Woods YL, Cohen P, Becker W, Jakes R, Goedert M, Wang X, Proud CG: **The kinase DYRK phosphorylates protein-synthesis initiation factor eIF2Bepsilon at Ser539 and the microtubule-associated protein tau at Thr212: potential role for DYRK as a glycogen synthase kinase 3-priming kinase.** *Biochemical Journal* 2001, **355**:609-615
35. Sontag E, Nunbhakdi Craig V, Bloom GS, Mumby MC: **A novel pool of protein phosphatase 2A is associated with microtubules and is regulated during the cell cycle.** *Journal of Cell Biology* 1995, **128**:1131-1144
36. Goldberg Y: **Protein phosphatase 2A: who shall regulate the regulator?** *Biochemical Pharmacology* 1999, **57**:321-328
37. Dunn B, Wobbe RC: **Introduction of DNA into yeast cells.** *In: Current Protocols in Molecular Biology Edited by Ausubel FM, Brent R, Kingston RE, Moore DD, Seidman JG, Smith JA, Struhl K, vol. 13.7.1. New York: John Wiley & Sons, Inc.;* 1993
38. Blom N, Gammeltoft S, Brunak S: **Sequence and structure-based prediction of eukaryotic protein phosphorylation sites.** *Journal of Molecular Biology* 1999, **294**:1351-1362